

FINITE-TEMPERATURE SU(2) LATTICE GAUGE THEORY WITH DYNAMICAL FERMIONS

U. HELLER

CERN, Geneva, Switzerland

F. KARSCH

*Department of Physics, University of Illinois at Urbana—Champaign, Urbana,
Illinois 61801, USA*

Received 21 January 1985

We study the influence of dynamical quarks on the deconfinement and chiral phase transitions of SU(2) lattice gauge theory using staggered fermions. The pseudo-fermion algorithm is used to include the effects of two flavours of light quarks in a Monte Carlo simulation on lattices of size $8^3 \times 2$ and $8^3 \times 4$. The systematic errors resulting from a truncation of the algorithm after a finite number of iterations are analyzed. In addition, we perform a weak coupling expansion of thermodynamic observables up to one-loop (order g^2) to study the high-temperature limit of the quark-gluon plasma.

1. Introduction

The chiral and deconfining phase transitions in SU(N) gauge theories have by now been studied in great detail in the pure gauge sector of the theories (for a recent review and references see [1]). In this sector the nature of the deconfinement transition is well understood in terms of the breaking of a global Z(N) symmetry present in the pure gauge models. In fact, the order of the phase transitions seen in Monte Carlo (MC) simulations agrees well with expectations based on universality arguments [2] and mean field analysis of effective Z(N) spin models [3].

In the presence of dynamical quarks the situation becomes more complicated. The global Z(N) symmetry of the pure gauge sector is explicitly broken by the fermions and is no longer associated with a deconfinement transition. The analysis of effective spin models [3, 4] and MC simulations with heavy quarks included via a hopping parameter expansion [5] suggest that the deconfinement transition in fact disappears for any finite quark mass in the case of SU(2) and below a critical mass for SU(N) with $N \geq 3$. On the other hand, the chiral transition is shown to be present in the zero mass limit [6]. It is thus a priori not clear how the phase transitions at zero and infinite mass (pure gauge theory) will influence the thermodynamic behaviour at

finite quark mass. MC simulations for the SU(3) theory show that even for finite quark masses a sudden change, perhaps even a phase transition, persists in thermodynamic quantities [7].

In this paper, we will investigate the thermodynamics of SU(2) gauge theory with two light-quark flavours. Firstly, we are interested in the phase structure of the SU(2) gauge theory in the presence of dynamical quarks. There is, however, another interesting feature of the influence of fermions on the thermodynamics of SU(N) gauge theories observed in the first SU(3) simulations, which we will address. It has been found that, unlike in the pure gauge theory, the energy density is far from showing asymptotic free gas behaviour even at rather high temperatures [7]. Moreover, the deviations from the Stefan-Boltzmann limit are positive, contrary to what one would expect from continuum perturbation theory [8]. It is thus important to understand whether the large deviations observed indicate the relevance of interactions in the quark-gluon plasma even at rather high temperatures, or whether they are due to finite-lattice-size effects. We will discuss this question in detail in sect. 3 where we give the results of an $O(g^2)$ (one-loop) weak coupling calculation of the energy density. This has been done previously in the pure gauge sector [9]. Our results indicate that finite-size effects are more severe in the presence of (staggered) quarks than in the pure gauge sector, where the correct $O(g^2)$ corrections have been observed on rather small lattices (see ref. [10] and also discussion in ref. [9]).

The following section, sect. 2, serves to fix our notations and gives the basic formulas for the discussion of the thermodynamics of SU(2) gauge theory with staggered fermions. In sect. 3, we discuss the results of an $O(g^2)$ weak coupling expansion. Our MC simulations on $8^3 \times 2$ and $8^3 \times 4$ lattices are discussed in sect. 4. Sect. 5 contains our conclusions. Some explicit formulae of the weak coupling expansion are given in an appendix.

2. Basic formulas for lattice thermodynamics

In the following we will discuss the thermodynamics of SU(2) lattice gauge theory in the presence of dynamical quarks. In order to preserve the chiral symmetry of the continuum theory, at least partially on the lattice, we used staggered fermions^{*}. The action is then defined as

$$S = S_G + S_F, \quad (1)$$

with

$$S_G = \beta \sum_{x, \mu < \nu} \left[1 - \frac{1}{2} \text{Tr} \left(U_{x, \mu} U_{x+\mu, \nu} U_{x+\nu, \mu}^\dagger U_{x, \nu}^\dagger \right) \right], \quad (2)$$

$$S_F = m \sum_x \bar{\chi}_x \chi_x + \frac{1}{2} \sum_{x, \mu} \bar{\chi}_x \eta_\mu(x) \left[U_{x, \mu} \chi_{x+\mu} - U_{x-\mu, \mu}^\dagger \chi_{x-\mu} \right]. \quad (3)$$

^{*} For a discussion of the symmetries of the staggered fermion action, see for instance [11].

Here $U_{x,\mu}$ are the usual gauge variables defined on the links of a hypercubic lattice of size $N_\sigma^3 \times N_\tau$. χ_x and $\bar{\chi}_x$ are the single-component Grassmann fields defined on the sites of the lattice. $\eta_\mu(x)$ are phase factors given by $\eta_\mu(x) = (-1)^{x_1 + \dots + x_{\mu-1}}$. The action depends on the bare quark mass m and the gauge coupling $\beta \equiv 4/g^2$. The partition function is then given as

$$Z = \int \prod_{x,\mu} dU_{x,\mu} \prod_x d\chi_x d\bar{\chi}_x e^{-S}. \quad (4)$$

The fermionic action, eq. (3), describes four flavours of mass m . After integration over the fermionic fields one obtains a fermion determinant, and the number of flavours can be varied formally by taking an appropriate power of this determinant:

$$Z = \int \prod_{x,\mu} dU_{x,\mu} \exp\left\{-S_G + \frac{1}{8}n_f \log \text{tr}(-D^2 + m^2)\right\}, \quad (5)$$

where $D = \sum_\mu D^\mu$ and

$$D_{x,y}^\mu = \frac{1}{2}\eta_\mu(x) \left[U_{x,\mu} \delta_{y,x+\mu} - U_{y,\mu}^\dagger \delta_{y,x-\mu} \right]. \quad (6)$$

The thermodynamics of the quark-gluon system can be studied by looking at order parameters and/or the behaviour of thermodynamic quantities. To this end we will analyze the chiral order parameter

$$\langle \bar{\psi}\psi \rangle = \langle \bar{\chi}\chi \rangle = \frac{1}{4}n_f \left\langle \text{tr}(D + m)_{x,x}^{-1} \right\rangle, \quad (7)$$

and the Polyakov line (thermal Wilson line), which is an order parameter for the deconfinement transition in the pure gauge theory ($m = \infty$)

$$\langle L \rangle = \left\langle \frac{1}{N_\sigma^3} \sum_x \frac{1}{2} \text{tr} \left(\prod_{x_4=1}^{N_\tau} U_{(x,x_4),4} \right) \right\rangle. \quad (8)$$

The energy density of the system can be written as

$$\varepsilon = \varepsilon_G + \varepsilon_F, \quad (9)$$

where ε_G , the ‘‘gluonic part’’, is given by

$$\varepsilon_G = 3\beta(\langle P_\sigma \rangle - \langle P_\tau \rangle), \quad (10)$$

with $\langle P_{\sigma,\tau} \rangle$ being the expectation values of space-space-like and space-time-like plaquettes. The ‘‘fermionic part’’ of the energy density, ε_F , is for gauge group SU(N)

$$\varepsilon_F = \frac{1}{4}n_f \left\langle \text{tr} D^4 (D + m)^{-1} \right\rangle - \left\{ \frac{1}{16} N n_f - \frac{1}{4} m \langle \bar{\psi}\psi \rangle_{T=U} \right\}. \quad (11)$$

The term in curly brackets in eq. (11) comes from normalizing the energy density by subtracting the zero-temperature contributions.

In the definition of the “gluonic part” of the energy density, we neglected contributions which result from the derivatives of the coupling with respect to the temperature [10]. These contributions, as verified at one value of β (see sect. 5), turn out to be small.

3. The high-temperature limit

The first MC simulations of the SU(3) lattice gauge theory with dynamical quarks showed that unlike in the pure gauge theory [1, 12] the energy density seems to approach the asymptotic Stefan-Boltzmann behaviour of an ideal gas from above showing considerable deviations even at rather high temperatures [7]. This is in contradiction to the expectations based on continuum perturbation theory where the $O(g^2)$ corrections are negative [8]. For massless quarks and the SU(N) colour group, the energy density is found to be

$$\epsilon/T^4 = \frac{1}{15}\pi^2\left((N^2 - 1) + \frac{7}{4}Nn_f\right) - \frac{1}{48}g^2(N^2 - 1)\left(N + \frac{5}{4}n_f\right). \quad (12)$$

However, higher-order corrections to eq. (12) have the opposite sign and it is therefore important to understand whether the MC data give evidence for a large contribution of higher-order corrections to the ideal gas behaviour even at rather high temperatures, or whether they indicate that the lattices used were too small to see the correct continuum behaviour.

To decide this question we performed an $O(g^2)$ weak coupling expansion of the energy density on finite lattices. The “gluonic part” ϵ_G , defined in eq. (10), has to a large extent been calculated in ref. [9]. It gets additional $O(g^2)$ contributions only from the fermionic contribution to the vacuum polarization. The plaquette expectation values are then given by

$$P_{\sigma,\tau} = g^2 \frac{(N^2 - 1)}{N} P_{\sigma,\tau}^{(2)} + g^4 (N^2 - 1) P_{\sigma,\tau}^{(4a)} + g^4 \frac{(2N^2 - 3)(N^2 - 1)}{N^2} P_{\sigma,\tau}^{(4b)} + g^4 n_f \frac{(N^2 - 1)}{N} P_{\sigma,\tau}^{(4f)} + O(g^6). \quad (13)$$

Here $P_{\sigma,\tau}^{(4f)}$ are the new contributions from the fermionic vacuum polarization effects. They are given in the appendix, while all the other expansion coefficients can be found in ref. [9]. The expansion of the “fermionic” part ϵ_F we parametrize as

$$\epsilon_F = n_f N \left(P_f^{(1)} + g^2 \frac{(N^2 - 1)}{N} P_f^{(2)} \right). \quad (14)$$

TABLE 1

The fermionic contributions to the $O(g^2)$ weak coupling expansion of the SU(N) energy density and $O(g^4)$ expectation value of the Polyakov line for staggered fermions of mass $ma = 0.1$

N_σ	N_τ	$P_\sigma^{(4f)}$	$P_\tau^{(4f)}$	$P_f^{(1)}$	$P_f^{(2)}$	$\epsilon_1^F/(N^2 - 1)$	$Q^{(4f)}$
8	2	$-4.0452 \cdot 10^{-4}$	$-8.7183 \cdot 10^{-4}$	$1.06784 \cdot 10^{-1}$	$-8.0036 \cdot 10^{-5}$	$2.7238 \cdot 10^{-3}$	$-2.5402 \cdot 10^{-3}$
	4	$-5.5491 \cdot 10^{-4}$	$-6.6229 \cdot 10^{-4}$	$7.03901 \cdot 10^{-2}$	$-2.4863 \cdot 10^{-4}$	$3.9565 \cdot 10^{-4}$	$-3.0619 \cdot 10^{-3}$
	6	$-5.8764 \cdot 10^{-4}$	$-6.1888 \cdot 10^{-4}$	$6.43231 \cdot 10^{-2}$	$-1.3187 \cdot 10^{-4}$	$5.5542 \cdot 10^{-5}$	$-3.1740 \cdot 10^{-3}$
12	2	$-4.0680 \cdot 10^{-4}$	$-8.9173 \cdot 10^{-4}$	$1.06654 \cdot 10^{-1}$	$-1.8639 \cdot 10^{-4}$	$2.7232 \cdot 10^{-3}$	$-3.6844 \cdot 10^{-3}$
	4	$-5.5905 \cdot 10^{-4}$	$-6.6443 \cdot 10^{-4}$	$7.00198 \cdot 10^{-2}$	$-2.8758 \cdot 10^{-4}$	$3.4471 \cdot 10^{-4}$	$-4.0540 \cdot 10^{-3}$
	6	$-5.9316 \cdot 10^{-4}$	$-6.1646 \cdot 10^{-4}$	$6.37634 \cdot 10^{-2}$	$-1.2474 \cdot 10^{-4}$	$1.5050 \cdot 10^{-5}$	$-3.7178 \cdot 10^{-3}$
8	2	$-5.9992 \cdot 10^{-4}$	$-6.0722 \cdot 10^{-4}$	$6.26108 \cdot 10^{-2}$	$-7.7905 \cdot 10^{-5}$	$-3.4064 \cdot 10^{-4}$	$-4.0595 \cdot 10^{-3}$
	4	$-5.9334 \cdot 10^{-4}$	$-6.6659 \cdot 10^{-4}$	$7.00047 \cdot 10^{-2}$	$-3.1695 \cdot 10^{-4}$	$3.2656 \cdot 10^{-4}$	$-5.0518 \cdot 10^{-3}$
	6	$-5.9367 \cdot 10^{-4}$	$-6.1674 \cdot 10^{-4}$	$6.37231 \cdot 10^{-2}$	$-1.3116 \cdot 10^{-4}$	$7.2785 \cdot 10^{-6}$	$-4.2909 \cdot 10^{-3}$
16	2	$-4.0696 \cdot 10^{-4}$	$-9.0214 \cdot 10^{-4}$	$1.06652 \cdot 10^{-1}$	$-2.5115 \cdot 10^{-4}$	$2.7199 \cdot 10^{-3}$	$-4.8239 \cdot 10^{-3}$
	4	$-5.5934 \cdot 10^{-4}$	$-6.6659 \cdot 10^{-4}$	$7.00047 \cdot 10^{-2}$	$-3.1695 \cdot 10^{-4}$	$3.2656 \cdot 10^{-4}$	$-5.0518 \cdot 10^{-3}$
	6	$-5.9367 \cdot 10^{-4}$	$-6.1674 \cdot 10^{-4}$	$6.37231 \cdot 10^{-2}$	$-1.3116 \cdot 10^{-4}$	$7.2785 \cdot 10^{-6}$	$-4.2909 \cdot 10^{-3}$
8	2	$-6.0064 \cdot 10^{-4}$	$-6.0698 \cdot 10^{-4}$	$6.25474 \cdot 10^{-2}$	$-7.6421 \cdot 10^{-5}$	$-3.8334 \cdot 10^{-5}$	$-4.4254 \cdot 10^{-3}$
	4	$-5.9334 \cdot 10^{-4}$	$-6.6659 \cdot 10^{-4}$	$7.00047 \cdot 10^{-2}$	$-3.1695 \cdot 10^{-4}$	$3.2656 \cdot 10^{-4}$	$-5.0518 \cdot 10^{-3}$
	6	$-5.9367 \cdot 10^{-4}$	$-6.1674 \cdot 10^{-4}$	$6.37231 \cdot 10^{-2}$	$-1.3116 \cdot 10^{-4}$	$7.2785 \cdot 10^{-6}$	$-4.2909 \cdot 10^{-3}$
20	10	$-6.0245 \cdot 10^{-4}$	$-6.0466 \cdot 10^{-4}$	$6.22640 \cdot 10^{-2}$	$-6.2050 \cdot 10^{-5}$	$-4.8758 \cdot 10^{-5}$	$-5.3079 \cdot 10^{-3}$

The expansion coefficients are defined in eqs. (13), (14) and (A.5). The explicit expressions are given in the appendix. Also listed is the complete fermionic $O(g^2)$ contribution ϵ_1^F defined in eq. (16d).

The explicit expressions are also given in the appendix where we further discuss the perturbative expansion of the expectation value of the Polyakov line, eq. (8).

The total energy of the quark-gluon gas on the lattice is now^{*}

$$\epsilon = \epsilon_0^G(N) + n_f \epsilon_0^F(N) + g^2 (\epsilon_1^G(N) + n_f \epsilon_1^F(N)), \quad (15)$$

where ϵ_i^G are the contributions from the pure gauge theory and ϵ_i^F are due to the effects of the dynamical fermions. They are given by

$$\epsilon_0^G(N) = 6(N^2 - 1)(P_\sigma^{(2)} - P_\tau^{(2)}), \quad (16a)$$

$$\epsilon_0^F(N) = NP_f^{(1)}, \quad (16b)$$

$$\epsilon_1^G(N) = 6N \left[(N^2 - 1)(P_\sigma^{(4a)} - P_\tau^{(4a)}) + \frac{(2N^2 - 3)(N^2 - 1)}{N^2} (P_\sigma^{(4b)} - P_\tau^{(4b)}) \right], \quad (16c)$$

$$\epsilon_1^F(N) = (N^2 - 1) [6(P_\sigma^{(4f)} - P_\tau^{(4f)}) + P_f^{(2)}]. \quad (16d)$$

^{*} In $O(g^2)$ there are additional contributions from the subtraction of the vacuum ($T = 0$) energy. These terms have been neglected here. Their contribution is small on lattices with small extent in the time direction. For discussion, see refs. [9,10]. The same is true for the flavour dependence of these terms. This has been discussed by Trinchero [13].

TABLE 2
Purely gluonic expansion coefficients of space-space-like (σ) and space-time-like (τ) plaquettes

N_σ	N_τ	$P_\sigma^{(2)}$	$P_\sigma^{(4a)}$	$P_\sigma^{(4b)}$	$P_\tau^{(2)}$	$P_\tau^{(4a)}$	$P_\tau^{(4b)}$
8	2	0.130788	$-2.94025 \cdot 10^{-4}$	$2.77555 \cdot 10^{-3}$	0.118968	$-9.1229 \cdot 10^{-5}$	$2.43426 \cdot 10^{-3}$
	4	0.125239	$-1.11582 \cdot 10^{-4}$	$2.60906 \cdot 10^{-3}$	0.124639	$-1.02366 \cdot 10^{-4}$	$2.59421 \cdot 10^{-3}$
	6	0.124994	$-1.03890 \cdot 10^{-4}$	$2.60332 \cdot 10^{-3}$	0.124925	$-1.03874 \cdot 10^{-4}$	$2.60162 \cdot 10^{-3}$
12	2	0.130903	$-3.41437 \cdot 10^{-4}$	$2.78018 \cdot 10^{-3}$	0.119025	$-7.1215 \cdot 10^{-5}$	$2.43689 \cdot 10^{-3}$
	4	0.125296	$-1.12495 \cdot 10^{-4}$	$2.61122 \cdot 10^{-3}$	0.124668	$-9.8312 \cdot 10^{-5}$	$2.59564 \cdot 10^{-3}$
	6	0.125034	$-1.02490 \cdot 10^{-4}$	$2.60479 \cdot 10^{-3}$	0.124942	$-1.02186 \cdot 10^{-4}$	$2.60254 \cdot 10^{-3}$
	8	0.125002	$-1.01926 \cdot 10^{-4}$	$2.60407 \cdot 10^{-3}$	0.124980	$-1.02098 \cdot 10^{-4}$	$2.60351 \cdot 10^{-3}$
16	2	0.130931	$-3.69635 \cdot 10^{-4}$	$2.78131 \cdot 10^{-3}$	0.119039	$-6.1333 \cdot 10^{-5}$	$2.43754 \cdot 10^{-3}$
	4	0.125310	$-1.14069 \cdot 10^{-4}$	$2.61175 \cdot 10^{-3}$	0.124675	$-9.6548 \cdot 10^{-5}$	$2.59599 \cdot 10^{-3}$
	6	0.125043	$-1.02337 \cdot 10^{-4}$	$2.60514 \cdot 10^{-3}$	0.124947	$-1.01603 \cdot 10^{-4}$	$2.60277 \cdot 10^{-3}$
	8	0.125009	$-1.01629 \cdot 10^{-4}$	$2.60433 \cdot 10^{-3}$	0.124983	$-1.01758 \cdot 10^{-4}$	$2.60368 \cdot 10^{-3}$
20	10	0.125004	$-1.01480 \cdot 10^{-4}$	$2.60423 \cdot 10^{-3}$	0.124993	$-1.01570 \cdot 10^{-4}$	$2.60397 \cdot 10^{-3}$

They are defined in eq. (13) and explicitly given in ref. [9].

The fermionic part still has to be normalized by subtracting the zero-temperature contributions (see eq. (11)). In table 1 we give the fermionic expansion coefficients $P_f^{(1)}$, $P_f^{(2)}$ and $P_{\sigma,\tau}^{(4f)}$ for various lattice sizes. Also included is $\epsilon_1^F/(N^2 - 1)$. As can be seen, the relative size of these expansion coefficients depends strongly on the (temporal) extent of the lattice. While for small N_τ the fermionic $O(g^2)$ contribution is positive, it becomes negative on larger lattices ($N_\tau \geq 8$) as expected from continuum perturbation theory. Table 2 is an extension of table 4 of ref. [9] giving the purely gluonic expansion coefficients for the same lattice sizes considered in table 1. In table 3 we finally give the lowest-order and $O(g^2)$ energy density for the SU(2) lattice gauge theory with two and four flavours of staggered fermions. There we have

TABLE 3
Lowest-order and $O(g^2)$ weak coupling SU(2) energy density for two and four flavours of staggered fermions of mass $ma = 0.1$

N_σ	N_τ	$n_f = 2$		$n_f = 4$	
		ϵ_0	ϵ_1/ϵ_0	ϵ_0	ϵ_1/ϵ_0
8	2	0.3899	0.06258	0.5670	0.07185
	4	0.04236	0.06398	0.07392	0.06878
12	6	$6.710 \cdot 10^{-3}$	0.02692	0.01176	0.02303

subtracted the zero-temperature contribution $\frac{1}{8}n_f$ of massless fermions. We find good agreement of this expansion with MC data.

One should notice, however, that the energy density given in table 3 and computed in MC experiments are not the complete expressions. There are additional contributions from the derivative terms (see refs. [9, 10]) and subtractions of vacuum terms. Only after taking into account these contributions will the correct perturbative continuum behaviour be recovered on the lattice. We have checked that this requires lattices with temporal size $N_\tau \geq 8$. The high-temperature behaviour observed in SU(2) and SU(3) simulations on lattices with $N_\sigma \leq 8$ and $N_\tau \leq 4$ is still largely influenced by finite-size effects.

4. SU(2) thermodynamics at intermediate temperatures

To study the thermodynamics of the quark-gluon system at intermediate temperatures we performed a MC simulation. The effects of dynamical fermion degrees of freedom in the gauge field updating have been included with the pseudo-fermion algorithm [14]. We performed simulations on lattices of size $8^3 \times 2$ and $8^3 \times 4$ for two quark flavours of identical mass. The fermion masses used were $ma = 0.1$ and 0.2 . For the pure gauge part of the action we used the icosahedral subgroup, and pseudo-fermionic scalar fields were updated with a heat-bath algorithm.

The pseudo-fermion algorithm introduces a two-fold bias in the evaluation of the (change in the) fermion determinant by assuming small changes in the gauge fields and by truncating the algorithm after a finite number of iterations. Since we used the icosahedral subgroup the minimal change of a gauge field (the one we used) was fixed by the distance between the unit matrix and the closest neighbours in the subgroup. These nearest neighbours have (Wilson) action $1 - \frac{1}{2}\text{tr } u = 0.194\dots$. We performed some trial runs with the full SU(2) group on a 4^4 lattice at $\beta = 2.2$ and found that this systematic effect is not very important. To check the influence of the truncation after a few steps we performed simulations with $N_{\text{PF}} = 60$ and 120 pseudo-fermion sweeps, neglecting the first 20 and 40 respectively before measuring averages. While for the larger mass, $ma = 0.2$, no systematic effects on expectation values of thermodynamic observables could be seen within the statistical errors, a clear systematic shift in all observables is visible for the smaller mass, $ma = 0.1$. This effect, however, decreases fast as the weak coupling region is approached. In fig. 1 we plot the relative change in $\langle \bar{\psi}\psi \rangle$:

$$\Delta(\bar{\psi}\psi) = \frac{\langle \bar{\psi}\psi \rangle_{120} - \langle \bar{\psi}\psi \rangle_{60}}{\langle \bar{\psi}\psi \rangle_{60}}, \quad (17)$$

where $\langle \dots \rangle_n$ denotes that n pseudo-fermion iterations have been used per gauge field update. As can be seen, for $\beta \geq 2.0$ no systematic deviations within the statistical errors are observable.

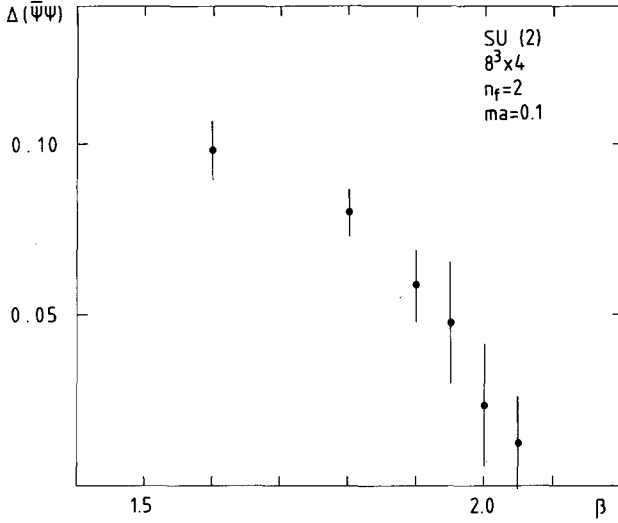


Fig. 1. Systematic deviations in the measurement of $\langle \bar{\psi}\psi \rangle$ on an $8^3 \times 4$ lattice due to the truncation of the pseudo-fermion algorithm after 60 and 120 iterations for two flavours of mass $ma = 0.1$. Shown is the relative change, eq. (17), based on 400 measurements for $N_{\text{PF}} = 120$ and 1500 for $N_{\text{PF}} = 60$ after 200 and 500 iterations respectively for equilibration.

Let us now discuss our MC results in more detail. They are based for the $8^3 \times 2$ lattice on 500 gauge field sweeps with the first 100 neglected for equilibration, while on the $8^3 \times 4$ lattice we performed 2000 iterations per data point and neglected the first 500. As starting configuration, the last one from a neighbouring β -value was used. At $\beta = 3.0$ we started from an ordered configuration, while at the lowest β -value we started from a completely random one.

Comparing the data on the $8^3 \times 2$ and $8^3 \times 4$ lattices, we see a clear difference in behaviour. While those for $N_\tau = 2$ are in general very smooth, giving no indication of a phase transition, the data for $N_\tau = 4$ show a rapid crossover in a narrow β -interval, $\beta \approx 2.0 \sim 2.1$, and are quite similar to results of the pure gauge theory. In fig. 2 we show the total energy density on both lattices. Since we had no data on symmetric (8^4) lattices except at $\beta = 2.3$ [15], we used the value of $\langle \bar{\psi}\psi \rangle$ on the asymmetric lattice in the normalization of the “fermionic” part of the energy density, eq. (11). At $\beta = 2.3$ the error introduced by this approximation is $\delta\epsilon a^4 = 1.7 \times 10^{-3}$ and 5×10^{-4} for $N_\tau = 2$ and 4 respectively, well within the statistical error. As mentioned in sect. 2, in the “gluonic” part of the energy density, we neglected contributions coming from the derivatives of the coupling with respect to the temperature [10]. These require the knowledge of the average plaquette on a symmetric lattice, which we only have at $\beta = 2.3$. There we find for these contributions $\delta\epsilon a^4 = -4.7 \times 10^{-2}$ and -2.9×10^{-3} for $N_\tau = 2$ and 4, i.e. an effect of about $\leq 10\%$, comparable to what one finds for the pure gauge theory.

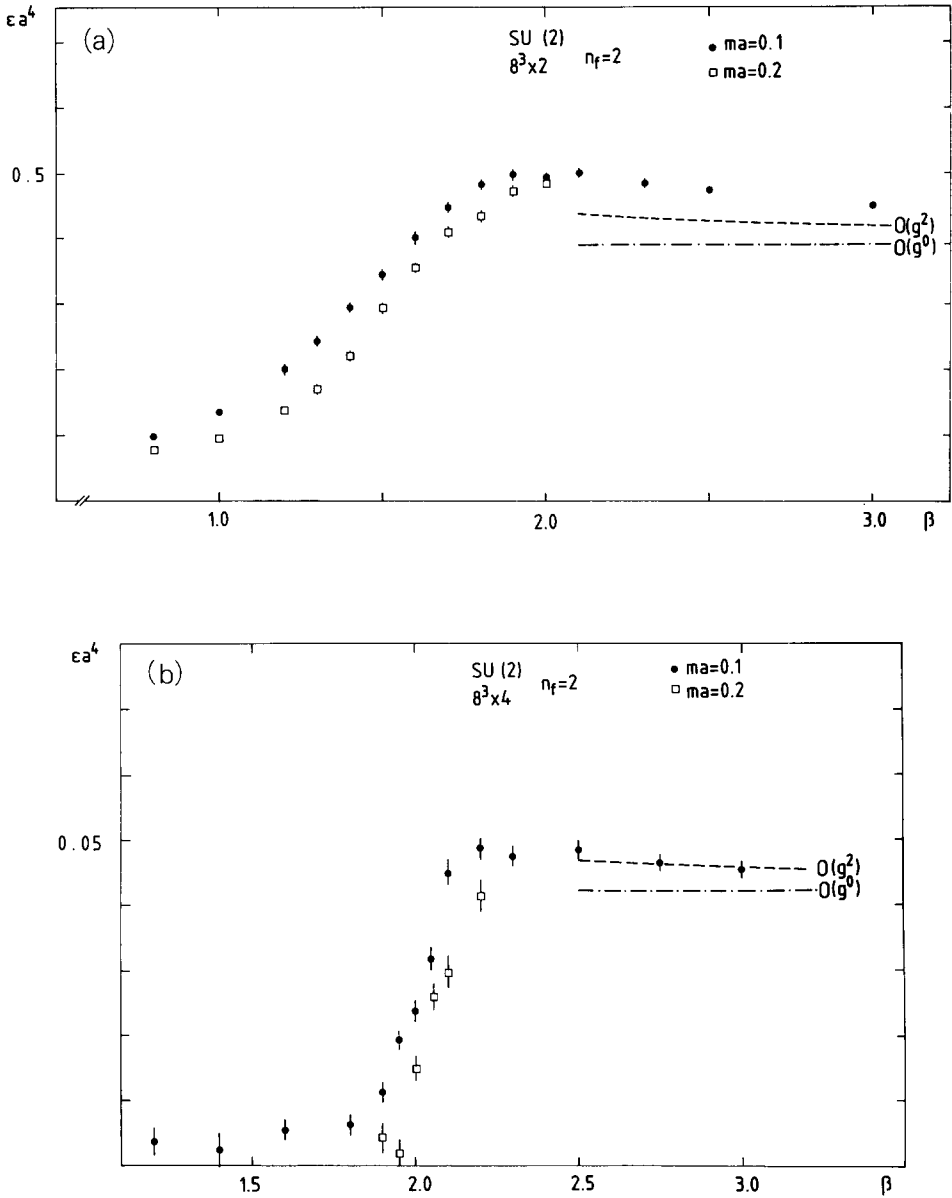


Fig. 2. The total energy density ϵa^4 of the quark-gluon system for two flavours of mass $ma = 0.1$ (●) and $ma = 0.2$ (□) as a function of β . (a) $8^3 \times 2$ lattice, (b) $8^3 \times 4$ lattice. Also shown are the lowest-order (— · —) and $O(g^2)$ (---) weak coupling results for ϵa^4 on lattices of the same size.

In the high-temperature region the MC data agree well with the perturbative expansion discussed in sect. 3. The smooth behaviour of the energy density for $N_\tau = 2$ might be an artifact of the too small temporal extent of the lattice. Recall that staggered fermions live effectively on a lattice with spacing $2a$. The bosonized action couples next to nearest neighbours and thus for $N_\tau = 2$ introduces an artificial self-coupling term.

A similar behaviour as for the energy density is found for the Polyakov line expectation value $\langle L \rangle$. This is shown in fig. 3, where we compare our data with $n_f = 2$ and mass $ma = 0.1$ and 0.2 with the pure gauge theory results of refs. [11, 16]. While $\langle L \rangle$ for $N_\tau = 2$ also shows no sign of a phase transition, the $N_\tau = 4$ data with and without dynamical fermions look very similar. This is shown again in fig. 4 where we plot the pure gauge theory results and our data on a shifted β -scale with a shift $\Delta\beta = 0.245$. The data for $\langle L \rangle$ show a tendency to become somewhat flatter for decreasing fermion mass. On the basis of the present data it is difficult to decide whether a phase transition persists for finite quark mass. For this a detailed finite size analysis of these observables would be necessary. We would expect that, as one increases N_σ , the tail of $\langle L \rangle$ at low β would become smaller and in the infinite volume limit disappear for the pure gauge theory, while with dynamical quarks this tail should persist due to the screening effects of the quarks. In any case our data give evidence that in the language of effective spin models, the influence of fermions even of mass $ma = 0.1$ corresponds to a rather small magnetic field.

The situation for the chiral order parameter seems to be clearer. On both lattices considered, $\langle \bar{\psi}\psi \rangle$ extrapolated linearly to zero mass varies rapidly and goes to zero (neglecting a finite tail, like in quenched calculations, which is believed to be due to finite-size effects) above a critical coupling. This is shown in fig. 5, where we plot $\langle \bar{\psi}\psi \rangle$ as extrapolated to zero from the $ma = 0.2$ data with $N_{\text{PF}} = 60$ and the $ma = 0.1$ with $N_{\text{PF}} = 120$. To illustrate the dependence of $\langle \bar{\psi}\psi \rangle$ on N_{PF} we used, on the $8^3 \times 4$ lattice, the values obtained at $ma = 0.1$ with $N_{\text{PF}} = 60$ and 120 and then extrapolated linearly in $1/N_{\text{PF}}$ to get an estimate for $\langle \bar{\psi}\psi \rangle$ with an infinite number of pseudo-fermion iterations. The value of the extrapolated $\langle \bar{\psi}\psi \rangle$ for zero mass obtained in this way is also shown in fig. 5b (crosses). As can be seen, this changes the slope of $\langle \bar{\psi}\psi \rangle$ but has little influence on the transition point (as was expected from fig. 1). We estimate for the critical coupling of chiral symmetry restoration

$$\beta_c(N_\tau = 2) = 1.65 \pm 0.1 \quad \text{for } N_\tau = 2,$$

$$\beta_c(N_\tau = 4) = 2.10 \pm 0.05 \quad \text{for } N_\tau = 4. \quad (18)$$

For the larger lattice the critical coupling is already in the region where approxi-

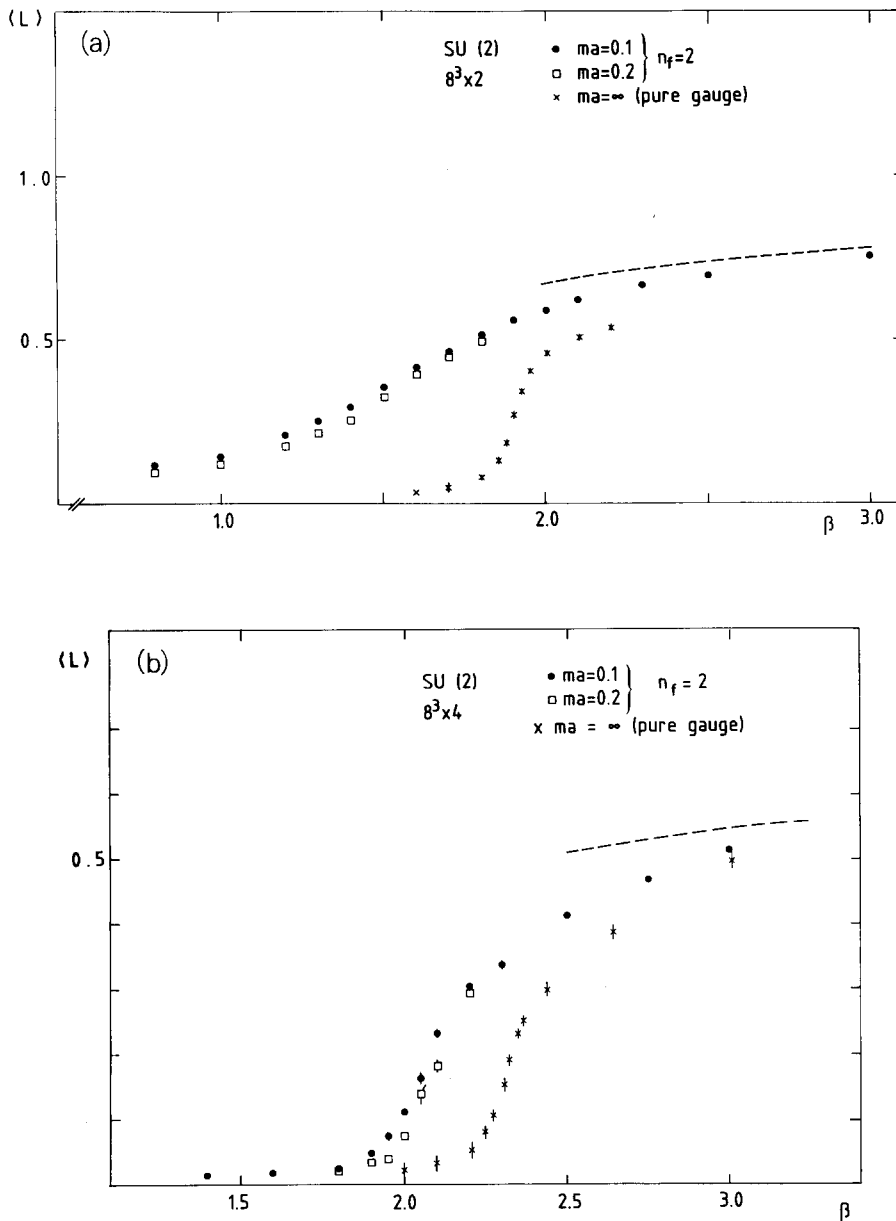


Fig. 3. The expectation value of the Polyakov line on an $8^3 \times 2$ (a) and $8^3 \times 4$ lattice (b) for the two-flavour system with mass $ma = 0.1$ (\bullet), 0.2 (\square) and ∞ , the pure gauge system (\times). Also shown is the $O(g^2)$ weak coupling result for $ma = 0.1$, discussed in the appendix.

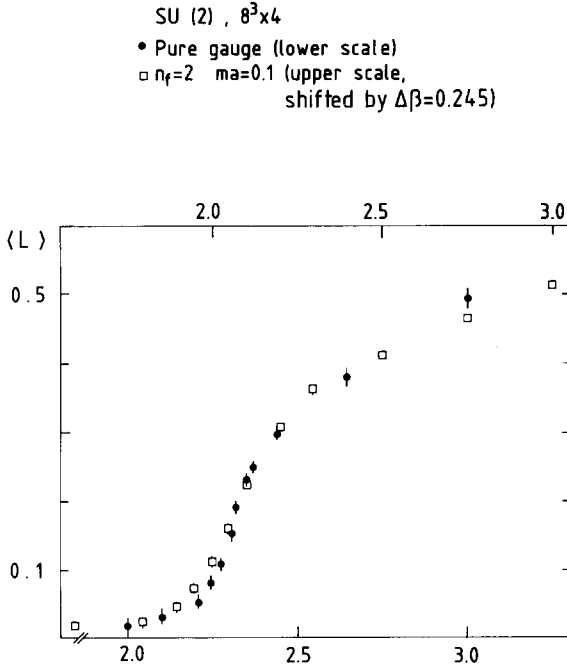


Fig. 4. Comparison of the Polyakov line expectation value on an $8^3 \times 4$ lattice for the pure gauge theory (●, lower scale) and two flavours of mass $ma = 0.1$ (□, upper scale) with β shifted by $\Delta\beta = 0.245$.

mately asymptotic scaling has been found for the two-flavour β -function [15]:

$$a\Lambda_L = \exp\left\{-\frac{1}{2b_0}g^{-2} - \frac{b_1}{2b_0^2}\log(b_0g^2)\right\},$$

$$b_0 = \frac{11N - 2n_f}{48\pi^2},$$

$$b_1 = \left(\frac{1}{16\pi^2}\right)^2 \left[\frac{34}{3}N^2 - \left(\frac{10}{3}N + \frac{N^2 - 1}{N}\right)n_f \right]. \quad (19)$$

Using this relation we find for the chiral transition temperature the estimate

$$T_{\text{CH}}/\Lambda_L = 87 \pm 14. \quad (20)$$

Using $\Lambda_{\text{min}}/\Lambda_L = 13.55$ for $n_f = 2$ [17] this becomes

$$T_{\text{CH}}/\Lambda_{\text{min}} = 6.4 \pm 1.1. \quad (21)$$

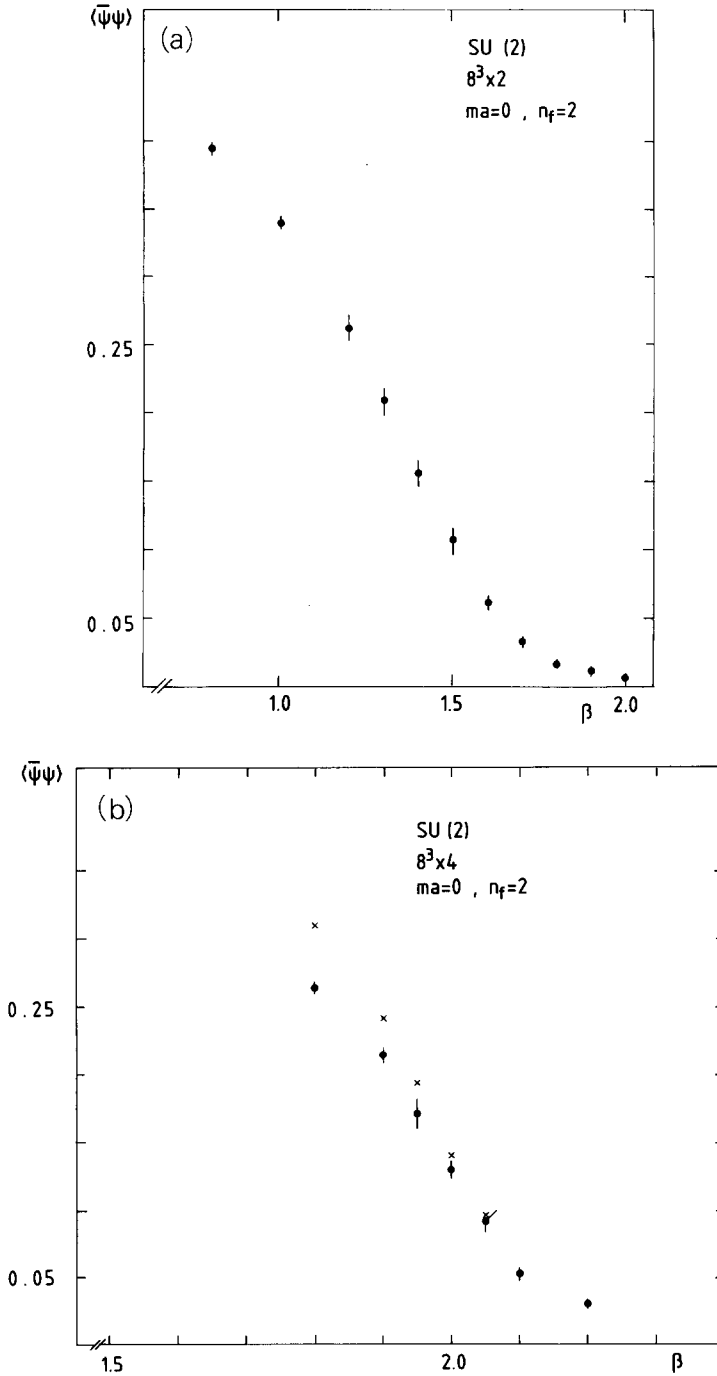


Fig. 5. The chiral order parameter on an $8^3 \times 2$ (a) and $8^3 \times 4$ lattice (b). Shown is $\langle \bar{\psi}\psi \rangle$ for two flavours as extrapolated linearly to $ma=0$ from data at $ma=0.1$ and 0.2 . In (b) the crosses in addition show the result for $\langle \bar{\psi}\psi \rangle_{m=0}$ when the $ma=0.1$ data are first extrapolated to an infinite number of pseudo-fermion sweeps.

To express T_{CH} in physical units, a measurement of a second physical quantity for the SU(2) two-flavour system is necessary. This has not yet been done.

5. Conclusions

We have studied the thermodynamics of the SU(2) lattice gauge theory with two flavours of staggered fermions. The high-temperature behaviour of the thermodynamic observables was found to be in agreement with $O(g^2)$ weak coupling perturbation theory on lattices of the same size as used in the MC simulations. The order- g^2 corrections in the weak coupling expansion are found to be strongly finite-size dependent and even change sign as the temporal extent, N_τ , of the lattice is increased. This explains the unexpected overshooting of the asymptotic free gas value observed for the energy density in SU(2) and SU(3) on small lattices.

At intermediate temperatures we find a clear signal for a chiral phase transition at vanishing quark mass. For intermediate masses the energy density and Polyakov line expectation value clearly still show a rapid change from high-temperature to low-temperature behaviour. Whether there is still a true phase transition cannot be unambiguously decided on the basis of the present data. This, we believe, would require an extensive finite-size analysis, much beyond our computer possibilities. However, we see indications that the observables, sensitive to a possible deconfinement transition, become smoother with decreasing quark mass. This makes it likely that the complete phase diagram for SU(2) agrees with the one expected from the effective spin models [3,4]: there are only true phase transitions at zero (chiral restoration) and infinite quark mass (deconfinement transition). Similar results as presented here for the two-flavour SU(2) theory have been obtained in the case of four flavours of staggered fermions using the microcanonical simulation method [18]. Our results for staggered fermions on the $8^3 \times 2$ lattice are also in agreement with results obtained with Wilson fermions on the same lattice size [19].

We would like to thank R. V. Gavai, P. Hasenfratz, J. Kogut, J. Polonyi and H. Satz for stimulating discussions.

Appendix

PERTURBATIVE CONTRIBUTIONS FROM FERMIONS

In this appendix we briefly describe the contributions from n_f flavours of Kogut-Susskind fermions up to second order in a weak coupling expansion of the quantities treated in this paper. The purely gluonic contributions can be found in ref. [9]. We use the notations introduced there ($f_p, s_p(p), \Delta_0$, etc.), with $L = N_\sigma$ and $L_d = N_\tau$. In addition we use the symbols

$$S_F(k) = \sum_{\mu} S_{\mu}^2(k) + m^2, \quad (\text{A.1})$$

and for the sum over the fermion momentum modes with antiperiodic boundary conditions in the time (d) direction:

$$\int_{k,\phi} = \frac{1}{L^{d-1}L_d} \sum_k \begin{cases} k_\mu = \frac{2\pi n_\mu}{L}, & 0 \leq n_\mu \leq \frac{1}{2}L - 1, \quad \mu \neq d \\ k_d = \frac{\pi(2n_d + 1)}{L_d}, & 0 \leq n_d \leq \frac{1}{2}L_d - 1. \end{cases} \quad (\text{A.2})$$

The perturbative treatment of the staggered fermions was done closely following ref. [17].

The fermions contribute to the expectation value of purely gluonic observables only through their contribution to the vacuum polarization tensor, which we find to be

$$\begin{aligned} \Pi_{\mu\nu}^{(\text{F})}(p) &\equiv g^2 n_f \tilde{\Pi}_{\mu\nu}^{(\text{F})}(p) \\ &= -g^2 n_f 2^{d/2-1} \delta_{\mu,\nu} \int_{k,\phi} \frac{s_\mu^2(k)}{S_{\text{F}}(k)} \\ &\quad + g^2 n_f 2^{d/2-1} \int_{k,\phi} \frac{c_\mu(\frac{1}{2}p+k) c_\nu(\frac{1}{2}p+k)}{S_{\text{F}}(k) S_{\text{F}}(p+k)} \\ &\quad \times \left[\delta_{\mu\nu} \left(\sum_\rho s_\rho(k) s_\rho(p+k) + m^2 \right) - 2s_\mu(k) s_\nu(p+k) \right]. \end{aligned} \quad (\text{A.3})$$

This gives rise to contributions $P_{\sigma,\tau}^{(4f)}$ to space-space and space-time plaquettes, defined in eq. (13), which are

$$\begin{aligned} P_\sigma^{(4f)} &= 2 \int_p \frac{1}{D(p)^2} \left\{ s_\nu^2(\frac{1}{2}p) \tilde{\Pi}_{\mu\mu}^{(\text{F})}(p) - s_\mu(\frac{1}{2}p) s_\nu(\frac{1}{2}p) \tilde{\Pi}_{\mu\nu}^{(\text{F})}(p) \right\}, \\ &\hspace{25em} \mu \neq \nu, \quad \mu, \nu \neq d, \\ P_\tau^{(4f)} &= \int_p \frac{1}{D(p)^2} \left\{ s_\mu^2(\frac{1}{2}p) \tilde{\Pi}_{dd}^{(\text{F})}(p) + s_d^2(\frac{1}{2}p) \tilde{\Pi}_{\mu\mu}^{(\text{F})}(p) \right. \\ &\quad \left. - 2s_\mu(\frac{1}{2}p) s_d(\frac{1}{2}p) \tilde{\Pi}_{\mu d}^{(\text{F})}(p) \right\}, \quad \mu \neq d. \end{aligned} \quad (\text{A.4})$$

Also the expectation value of Polyakov lines gets a new contribution. They now have

the expansion

$$\begin{aligned} \langle L \rangle = & 1 - g^2 \frac{N^2 - 1}{N} Q^{(2)} - g^4 (N^2 - 1) Q^{(4a)} \\ & - g^4 \frac{(2N^2 - 3)(N^2 - 1)}{N^2} Q^{(4b)} - g^4 n_f \frac{N^2 - 1}{N} Q^{(4f)} + O(g^6). \end{aligned} \quad (\text{A.5})$$

The coefficients $Q^{(2)}$, $Q^{(4a)}$ and $Q^{(4b)}$ can be found in ref. [9] and $Q^{(4f)}$ is

$$Q^{(4f)} = \frac{1}{4} L_d \int_p \frac{\tilde{\Pi}_{dd}^{(F)}(p)}{D(p)^2}. \quad (\text{A.6})$$

$Q^{(4f)}$ is given for a few lattices in table 1.

A little more involved is the perturbative computation of the fermionic part of the energy density, eq. (11). We find the expansion coefficients defined in eq. (14) as

$$P_f^{(1)} = 2^{d/2} \int_{k, \phi} \frac{s_d^2(k)}{S_F(k)}, \quad (\text{A.7})$$

$$\begin{aligned} P_f^{(2)} = & 2^{d/2-2} \Delta_0 \int_{k, \phi} \left[\frac{s_d^2(k) \left(\sum_{\rho} s_{\rho}^2(k) - m^2 \right)}{S_F(k)^2} - \frac{s_d^2(k)}{S_F(k)} \right] \\ & + 2^{d/2-1} \int_p \int_{k, \phi} \frac{s_d(k) s_d(k+p) \left[\sum_{\rho} c_{\rho}^2(\frac{1}{2}p+k) - 2c_d^2(\frac{1}{2}p+k) \right]}{D(p) S_F(k) S_F(p+k)} \\ & - 2^{d/2} \int_p \int_{k, \phi} \frac{s_d^2(k) \sum_{\rho} c_{\rho}^2(\frac{1}{2}p+k) \left[\sum_{\sigma} s_{\sigma}(k) s_{\sigma}(p+k) + m^2 - 2s_{\rho}(k) s_{\rho}(p+k) \right]}{D(p) S_F(k)^2 S_F(p+k)} \\ & + 2^{d/2-1} \int_p \int_{k, \phi} \frac{c_d^2(\frac{1}{2}p+k) \left[\sum_{\rho} s_{\rho}(k) s_{\rho}(p+k) + m^2 - 2s_d(k) s_d(p+k) \right]}{D(p) S_F(k) \cdot S_F(p+k)}. \end{aligned} \quad (\text{A.8})$$

Note that in all the formulas the dependence on the number of colours, N , and the number of flavours, n_f , has been explicitly exhibited.

References

- [1] F. Karsch, The deconfinement transition in finite temperature lattice gauge theory, preprint CERN-TH.4003 (1984)
- [2] B. Svetitsky and L.G. Yaffe, Nucl. Phys. B210 [FS6] (1982) 423
- [3] J. Bartholomew, D. Hochberg, P.H. Damgaard and M. Gross, Phys. Lett. 133B (1983) 218; F. Green and F. Karsch, Nucl. Phys. B238 (1984) 297
- [4] T. Banks and A. Ukawa, Nucl. Phys. B225 [FS9] (1983) 145
- [5] P. Hasenfratz, F. Karsch and I.O. Stamatescu, Phys. Lett. 133B (1983) 221
- [6] E.T. Tomboulis and L.G. Yaffe, Phys. Rev. Lett. 52 (1984) 2115
- [7] T. Celik, J. Engels and H. Satz, Phys. Lett. 133B (1984) 427; R.V. Gavai, M. Lev and B. Peterson, Phys. Lett. 140B (1984) 397; Bielefeld preprint BI-TP 84/10 (1984); F. Fucito, C. Rebbi and S. Solomon, CALTECH preprint CALT-68-1124 (1984); Nucl. Phys. B248 (1984) 615; J. Polonyi, H.W. Wyld, J.B. Kogut, J. Shigemitsu and D.K. Sinclair, Phys. Rev. Lett. 53 (1984) 644
- [8] J.I. Kapusta, Nucl. Phys. B148 (1979) 461; O.K. Kalshnikov and V.V. Klimov, Phys. Lett. 88B (1979) 328
- [9] U. Heller and F. Karsch, Nucl. Phys. B251 [FS13] (1985) 254
- [10] J. Engels, F. Karsch, I. Montvay and H. Satz, Nucl. Phys. B205 [FS5] (1982) 545
- [11] J. Kogut, M. Stone, H.W. Wyld, S. Shenker, J. Shigemitsu and D.K. Sinclair, Nucl. Phys. B225 [FS9] (1983) 326
- [12] J. Engels and F. Karsch, Phys. Lett. 125B (1983) 481
- [13] R. Trincherio, Nucl. Phys. B227 (1983) 61
- [14] F. Fucito, E. Marinari, G. Parisi and C. Rebbi, Nucl. Phys. B180 [FS3] (1981) 369; H.W. Hamber, E. Marinari, G. Parisi and C. Rebbi, Phys. Lett. 124B (1983) 99
- [15] U. Heller and F. Karsch, Phys. Rev. Lett. 54 (1985) 1765
- [16] R.V. Gavai and H. Satz, Phys. Lett. 145B (1984) 248
- [17] H.S. Sharatchandra, H.J. Thun and P. Weisz, Nucl. Phys. B192 (1981) 205
- [18] J. Kogut, J. Polonyi and H.W. Wyld, in preparation
- [19] A. Nakamura, Phys. Lett. 149B (1984) 391